

Signal Design for Bandwidth-Efficient Multiple-Access Communications Based on Eigenvalue Optimization

Tommy Guess, *Member, IEEE*, and Mahesh K. Varanasi, *Senior Member, IEEE*

Abstract—Bandwidth-Efficient Multiple Access (BEMA) is a strategy where transmitter pulses are continually designed at the base station and are dynamically allocated to the transmitters via a feedback channel. Such pulses (or “signature waveforms”) are designed to conserve bandwidth while simultaneously enabling the receiver at the base station to meet a Quality-of-Service (QoS) specification for each transmitter. The key technical problem in BEMA communication is therefore the design of the transmitter pulses for the base-station receiver. In an earlier paper [1], we presented solutions to this problem that were shown to be superior (in terms of strict bandwidth) to common signaling schemes such as Time-, Frequency-, and Code-Division Multiple Access (TDMA, FDMA, and CDMA). This paper uses the framework developed in [1], but considers strictly time-limited transmitter pulses and the root-mean squared (rms) bandwidth measure. As in [1], significant bandwidth savings over the traditional multiple-access strategies are obtained. However, in contrast to the rank-conserving approach of [1], the bandwidth gains of this paper are realized by tailoring the signature waveform design to conserve rms bandwidth via eigenvalue-optimization problems.

Index Terms—Bandwidth, decision feedback, multiaccess communication, multiuser channel, Quality-of-Service, signal design.

I. INTRODUCTION

A CORRELATED-Waveform Multiple-Access (CWMA) channel is defined in this work as a multiple-access channel wherein transmitters independently send digital information by means of pulse-amplitude modulation (PAM) with transmitter pulses that are allowed to be distinct for each user. In particular, if the transmitters employ orthogonal waveforms that are nonoverlapping in time or frequency, the CWMA system models Time-Division Multiple Access (TDMA) or Frequency-Division Multiple Access (FDMA), respectively. In practice, such multiple-access schemes are implemented in a dynamic fashion, where time or frequency slots are assigned to a transmitter when that transmitter has a message to transmit.

If the transmitter pulses are spread-spectrum signals of the direct-sequence or frequency-hop type, then the resulting strategy is called a Spread-Spectrum or Code-Division Multiple-Access (SSMA or CDMA) system. A dynamic version of a CDMA system is one where a predesigned spread-spectrum “code” is dynamically assigned to a transmitter whenever it has a message to transmit. A multiple-access technique which assigns identical waveforms to all users will henceforth be referred to as the Identical-Waveform Multiple Access (IWMA) channel.

A fundamental aspect in which the aforementioned multiple-access techniques differ is in the manner in which each allocates the expansion of bandwidth (relative to that required in a single-user channel) between “spreading” and error-control coding. Spreading is a term we use to denote the bandwidth expansion that is attributable to the use of distinct transmitter waveforms. For instance, TDMA and FDMA employ orthogonal transmitter pulses to separate the users and so the spreading factor is equal to the number of users (in practice, it is actually somewhat higher to create guard times and guard bands). In IWMA there is no spreading (i.e., the spreading factor is unity) and it thus relies entirely on coding to separate the users. For CDMA, spreading factors are generally understood to be much higher than the number of users.

A CWMA system must be understood as one that does not *a priori* impose any particular structure on the transmitter waveforms and as such includes TDMA, FDMA, CDMA, or IWMA as particular cases. We assume that traffic conditions (e.g., the number of active transmitters, their received powers, etc.) remain relatively unchanged over a sufficiently large number of transmitted symbols. It is then possible to dynamically maximize the performance of the CWMA channel over the transmitter pulses subject to bandwidth constraints to obtain an optimal multiaccess scheme. For instance, the total capacity or the maximum achievable sum-rate of the transmitters was optimized under an rms bandwidth constraint for the two-user channel by Cheng and Verdú in [2] and algorithms for constructing the optimal signature waveforms for the general K -user channel were obtained by Parsavand and Varanasi in [3] for both the equal and unequal received power cases. The same performance criterion was optimized under a constraint on the spreading gain by Rupf and Massey in [4] for the case of equal received powers, and by Viswanath and Anantharam in [5] for the case of unequal received powers, along with a recursive algorithm to construct the corresponding signature sequences. More recently, algorithms for constructing signature waveforms and power-allocation strategies that optimize total

Manuscript received December 1, 1998; revised July 24, 1999. This work was supported in part by the National Science Foundation under Grant NCR-9706591. The material in this paper was presented in part at the Communication Theory Mini-Conference (CTMC) of the International Conference on Communication (ICC'99), Vancouver, BC, Canada, June 7–9, 1999.

T. Guess is with the Department of Electrical Engineering, University of Virginia, Charlottesville, VA 22904-4743 USA (e-mail: trg6f@virginia.edu).

M. K. Varanasi is with the Department of Electrical and Computer Engineering, University of Colorado, Boulder, CO 80309-0425 USA (e-mail: varanasi@schof.colorado.edu).

Communicated by M. L. Honig, Associate Editor for Communications.

Publisher Item Identifier S 0018-9448(00)06988-1.

capacity under the location-invariant fractional out-of-band power (FOBP) and rms bandwidth criteria were obtained by Varanasi and Fain in [6].

Signal design based on a Quality-of-Service (QoS) criterion was proposed by Varanasi and Guess in [7], [1]. It represents a more practical approach to the joint transmitters–receiver design problem in a multiple-access channel. The objective in [1] was to obtain infinite-duration signals occupying as little strict bandwidth as possible while meeting a QoS specification for each user. In this paper, we seek strictly time-limited signals that are bandwidth-efficient in terms of the rms bandwidth measure. As in [1], we will focus on decision-feedback receivers (DFRs) and consider, in particular, the popular but suboptimal successive canceler, the zero-forcing (ZF) DFR, and the capacity-maximizing (CM) DFR (or, equivalently, the maximum signal-to-interference ratio (MSIR) DFR [8]).

The multiple-access strategy in which signals are designed to conserve bandwidth while meeting a QoS objective for each user has been dubbed Bandwidth-Efficient Multiple Access (BEMA) in [1]. In a related work, a QoS-based approach to signature sequence design (with power control) for the suboptimal linear Minimum Mean-Square Error (MMSE) and matched-filter detectors under a constraint on spreading gain was considered by Viswanath, Anantharam, and Tse in [9]. A distributed algorithm that converges to the optimal sequences found therein was obtained by Ulukus and Yates in [10].

The rest of this paper is organized as follows. Section II contains an introduction to BEMA and the formulation and reduction of the problem of central interest in this paper. This includes the CWMA system model, its rms bandwidth, and a brief description of the decision-feedback receivers for which signals are to be designed, along with formulas for their signal-to-interference ratios (SIRs). Rather than considering the bandwidth-minimization problem, which appears to be intractable, we describe a suboptimal greedy algorithm for which we state the QoS constraint on the SIRs of the decision-feedback receivers for each user. The rest of the paper deals with the problem of designing signals that conserve bandwidth while satisfying the QoS constraints. In particular, Section III and the Appendix obtain solutions to certain eigenvalue-optimization problems and develop key properties of the constraint sets that impact bandwidth conservation. Section IV uses the results of Section III to prescribe the new signal-design methodology. Section V contains numerical examples to illustrate the advantages of this BEMA design over IWMA and TDMA. Section VI concludes this paper.

II. BANDWIDTH-EFFICIENT MULTIPLE ACCESS

BEMA is an adaptive signaling strategy for multiaccess communications. Transmitter pulses or signature waveforms are continually computed at the base station as a function of the multiuser receiver employed there, and the traffic conditions such as received power levels, number of active transmitters, etc. They are then dynamically allocated from the central receiver to the transmitters at a frequency that is dictated by the rate of significant change of those conditions. Our work here applies to multiple-access channels in which this change takes

place sufficiently slowly (relative to the data rate) so as to allow effective adaptation.

This section formulates and simplifies the joint transmitter–receiver design problem for BEMA communications. It describes the CWMA channel model and contains a discussion of bandwidth measures including, in particular, the rms bandwidth. While the results of this paper are obtained in the context of rms bandwidth, the techniques developed herein are applicable to a variety of other bandwidth measures as well. Three DFRs are specified, namely, the successive cancellation based DFR, the ZF-DFR, and the CM-DFR. As for the QoS constraints, each user effectively sees a single-user channel, as yielded by the particular DFR, of some prespecified SIR. This SIR depends on the DFR used and the correlation matrix of the signature signals of the transmitting users. A procedure for obtaining the transmitter pulses is proposed via a construction of their correlation matrix wherein the correlations between the users' signals are obtained in the reverse of the order in which the users are decoded. The addition of a user corresponds to incrementing the dimension of the correlation matrix by one. The constraint that the enlarged correlation matrix be positive semidefinite at each step is stated here for each of the three DFRs without proof. The two key results in this section on the SIRs of decision feedback receivers (DFRs) and the positive semidefinite constraint were proved by the authors in [11] and [1], respectively. Those results are summarized here in order to properly formulate the rms signal-design problem and to motivate the eigenvalue-optimization approach.

A. The CWMA System

In a CWMA channel, K users transmit PAM waveforms simultaneously. It is assumed that the received signal is the symbol-synchronous superposition of these waveforms that has been corrupted by additive white Gaussian noise (AWGN). Thus

$$y(t) = \sum_n \sum_{k=1}^K X_k(n) u_k(t - nT) + n(t) \quad (1)$$

where $\{X_k(n)\}_n$ is the independent and identically distributed (i.i.d.) sequence of information symbols sent by the k th user, $u_k(t)$ is the signature waveform of the k th user assumed to be time-limited to the symbol duration $[0, T]$ and normalized to have unit energy, and $n(t)$ is an AWGN process with a two-sided power spectral density of $N_0/2$. If the power of the k th user's signature waveform is constrained to be w_k , then without loss of generality it can be assumed that $\frac{1}{T} E\{X_k^2(n)\} = w_k$ for each k . The correlation matrix of the signature waveforms is denoted as \mathbf{R} where its (i, j) th element is given as $R_{ij} = \int_0^T u_i(t) u_j(t) dt$ and the unit-energy normalization implies that $R_{kk} = 1$ for all k . We let $\mathbf{W} = \text{diag}(w_1, w_2, \dots, w_K)$ denote the diagonal matrix of the users' powers. The weighted correlation matrix is defined as $\mathbf{H} = \mathbf{W}^{1/2} \mathbf{R} \mathbf{W}^{1/2}$.

Sampling at integer multiples of T , the outputs of a bank of filters matched to each of the signature waveforms yields sufficient statistics so that the equivalent discrete-time model is

$$\mathbf{Y}(n) = \mathbf{R} \mathbf{X}(n) + \mathbf{N}(n) \quad (2)$$

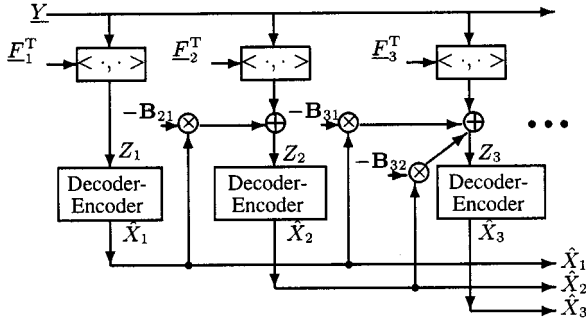


Fig. 1. The decision-feedback receiver.

where $\underline{X}(n)$ is the vector of information symbols of the users at time n and $\{\underline{N}(n)\}$ is a sequence of i.i.d. zero-mean, Gaussian random vectors, each with covariance $\frac{N_0}{2} \mathbf{R}$.

B. Bandwidth Measures

We consider the root-mean squared (rms) bandwidth which measures the standard deviation of the power spectral density of the superposition of the users' transmitted waveforms. Given the users' weighted correlation matrix \mathbf{H} , it was shown in [3] that there exists a corresponding set of minimum-bandwidth signature waveforms for which the rms bandwidth of the superposition depends on \mathbf{H} only through a linear combination of its eigenvalues [3]. This minimum bandwidth can be expressed as $\sum_{k=1}^K c_k \lambda_k$, where $\lambda_1 \geq \lambda_2 \geq \dots \geq \lambda_K$ are the eigenvalues of \mathbf{H} arranged in a nonincreasing order, and the nonnegative constants $0 \leq c_1 \leq c_2 \leq \dots \leq c_K$ are arranged in the nondecreasing order. Remarkably, there are other measures such as the fractional out-of-band power (FOBP) and fourth-moment bandwidths that have the same functional form [6], [12]. Consequently, while the specific values of the constants differ from one measure to another, as do the basis functions that must be used to construct the signature waveforms from their correlation matrix, the design methodology presented here can be used for all such measures of bandwidth that possess the aforementioned characteristic. In particular, [3, Proposition 7] shows that the minimum rms bandwidth is a function of $\sum_{k=1}^K k^2 \lambda_k$ and is given as

$$B_{\text{rms}} = \frac{1}{2T} \sqrt{\sum_{k=1}^K \frac{k^2 \lambda_k}{\text{trace}(\mathbf{W})}}. \quad (3)$$

C. Decision-Feedback Receivers

In this section, we describe DFRs for coded systems (with an uncoded system viewed as a special case). A DFR (cf. [7]) decodes users sequentially as illustrated in Fig. 1. It is parameterized by a $K \times K$ feedforward and feedback matrix pair (\mathbf{F}, \mathbf{B}) , where \mathbf{B} is strictly lower-triangular.

The first user is decoded based on Z_1 , which is obtained by taking the inner product between the first row of \mathbf{F} , which we denote by \underline{F}_1^T , and the matched-filter output vector \underline{Y} . The decoded output is re-encoded to produce \hat{X}_1 . The second user is

decoded based on Z_2 , where Z_2 is obtained by first performing an inner product between \underline{F}_2^T and the output \underline{Y} , and then subtracting from it a scalar multiple B_{21} (i.e., the $(2, 1)$ element of \mathbf{B}) times the decoded and re-encoded symbol \hat{X}_1 of the first user. In general, the k th user is decoded based on

$$Z_k = \underline{F}_k^T \underline{Y} - \sum_{j=1}^{k-1} B_{kj} \hat{X}_j.$$

Note that decoding delays are not shown in Fig. 1.

When feedback is assumed to be perfect, an assumption that is in principle justified (for any order of decoding) since the joint error rate, defined as the probability that at least one user is decoded incorrectly, of a decision feedback receiver, with and without the perfect feedback assumption, are equal (cf. [13] [14]),¹ the optimal \mathbf{B} is the strictly lower-triangular part of \mathbf{FR} (henceforth denoted as $\mathcal{L}(\mathbf{FR})$). This expurgates "past" users, i. e., users 1 to $k-1$, before the k th user is decoded. The effective channel seen by the k th user is a memoryless, single-user channel that is characterized by the SIR of this user, which we denote by γ_k .

As for the QoS constraints, we require that γ_k , the SIR of the k th user's channel, be greater than a preset threshold for that user.²

The results of this paper readily apply to uncoded systems as well. In fact, it is to this context that we shall focus our attention in much of this paper. For uncoded transmissions, the decoder–encoder blocks of Fig. 1 are replaced by symbol-by-symbol decision rules for the particular modulation schemes used [7] (such as PAM or QAM quantizers). In order for the assumption of perfect feedback to be reasonable in this case, however, users must be decoded in the decreasing order of their QoS requirements (cf. [13]). We return to this issue in the next subsection.

Three DFRs are of particular interest (they are described in detail in [7]). For successive cancellation there is no feedforward equalization so that $\mathbf{F} = \mathbf{I}$ and $\mathbf{B} = \mathcal{L}(\mathbf{R})$. The zero-forcing (ZF) DFR decorrelates future users so that $\mathbf{F} = (\mathbf{\Phi}^T)^{-1} \mathbf{W}^{1/2}$ and $\mathbf{B} = \mathcal{L}(\mathbf{\Phi}) \mathbf{W}^{-1/2}$, where the lower-triangular matrix $\mathbf{\Phi}$ arises from the Cholesky decomposition $\mathbf{H} = \mathbf{\Phi}^T \mathbf{\Phi}$. Finally, the capacity-maximizing (CM) DFR is specified by $\mathbf{F} = (\mathbf{\Psi}^T)^{-1} \mathbf{W}^{1/2}$ and $\mathbf{B} = \mathcal{L}(\mathbf{\Psi}) \mathbf{W}^{-1/2}$, where $\mathbf{\Psi}$ is the lower-triangular matrix that results from the Cholesky factorization $\mathbf{\Psi}^T \mathbf{\Psi}$ of the matrix $\mathbf{H} + \sigma^2 \mathbf{I}$. Note that in all cases, $\mathbf{B} = \mathcal{L}(\mathbf{FR})$. In a coded system, the CM-DFR has the important property that it achieves the total capacity of the CWMA channel with single-user coding and decoding, as was shown by the authors in [8].

We will use the following notation regarding \mathbf{H} . Let $\mathbf{H}_{(k)}$ denote the principal submatrix of \mathbf{H} formed by indices k through

¹As a result, each user's error rate is upper-bounded by the sum of the error rates of the corresponding perfect-feedback DFR for that user and the previously decoded users. Hence, each user's code can be chosen to be sufficiently long so as to impact the future user error rates via error propagation as negligibly as we please.

²The capacity of the k th user's channel under the assumption of Gaussian input symbols (which are optimal in terms of maximizing the capacity region) and perfect feedback, is given as $C_k = \frac{1}{2T} \log(1 + \gamma_k)$, which for fixed T , is monotonically increasing in γ_k .

K , and let $\underline{H}_{(k)}^T$ denote the row vector $[H_{kk+1} \dots H_{kK}]$. That is,

$$\mathbf{H}_{(k)} = \begin{bmatrix} w_k & \underline{H}_{(k)}^T \\ \underline{H}_{(k)} & \mathbf{H}_{(k+1)} \end{bmatrix}. \quad (4)$$

The SIRs achieved by the k th user for each of the three DFRs are summarized in the lemma below.

Lemma 1:

$$\gamma_k = \begin{cases} \sigma^{-2} w_k^2 (w_k + \underline{H}_{(k)}^T (\sigma^2 \mathbf{I})^{-1} \underline{H}_{(k)})^{-1} & \text{Suc. Cancel.} \\ \sigma^{-2} (w_k - \underline{H}_{(k)}^T (\mathbf{H}_{(k+1)})^{-1} \underline{H}_{(k)}) & \text{ZF-DFR} \\ \sigma^{-2} (w_k - \underline{H}_{(k)}^T (\mathbf{H}_{(k+1)} + \sigma^2 \mathbf{I})^{-1} \underline{H}_{(k)}) & \text{CM-DFR.} \end{cases} \quad (5)$$

The result for the CM-DFR is proved in [1]. The SIRs of the ZF-DFR and successive cancellation can be obtained similarly.

D. Signal Design

The signal-design problem is this: given a fixed set of received powers and the order in which users are decoded, find the transmitter pulses that result in a bandwidth of the superposition of transmitted waveforms that is as small as possible while enabling an arbitrary decision-feedback receiver ($\mathbf{F}, \mathbf{B} = \mathcal{L}(\mathbf{FR})$) at the base station to meet a target SIR criterion for each user. We assume no power control so that the received powers can be similar or widely disparate depending on the geographical distribution of the transmitters relative to the base station. To specify the target SIRs we require that

$$\gamma_k \geq \beta_k \triangleq \frac{\eta_k w_k}{\sigma^2} \quad (6)$$

where $\eta_k \in (0, 1]$ for each k . That is, the k th user's target SIR is a fraction of that user's SNR if there were no interfering users. Implicit here is the reasonable assumption that each user's power is sufficiently high so that if that user were the only one transmitting, then its data would be satisfactorily decoded.

1) *Bounds on Minimum Bandwidth:* The problem of finding the transmitter pulses that yield minimum bandwidth while satisfying the SIR constraints appears to be analytically intractable. This is because the rms bandwidth as given by (3) is related to the users' SIRs in (5) in some complicated way that is not easily amenable to its optimization. In this section, we find bounds on the minimum bandwidth and use them as benchmarks for our signal design method.

For an upper bound, we simply use the minimum bandwidth needed for orthogonal signaling (which clearly satisfies the SIR constraints for any one of the three DFRs). Users are assigned orthogonal sinusoidal signals and we will henceforth refer to this simple strategy as optimal-orthogonal multiple access (OOMA). Its bandwidth is obtained by substituting $\mathbf{H} = \mathbf{W}$ into (3). Hence, there must exist signal sets that

satisfy the SIR constraints for any one of the three DFRs with a time-bandwidth product that is upper-bounded as

$$BT \leq \frac{1}{2} \sqrt{\frac{\sum_{k=1}^K w_k k^2}{\sum_{k=1}^K w_k}}. \quad (7)$$

A trivial lower bound on BT is $\frac{1}{2}$. This lower bound is unachievable except in situations for which the QoS constraints are such that a DFR is able to meet them for IWMA.

In the case of the ZF-DFR, we derive a lower bound that is often tighter than this trivial bound. We have that

$$BT = \frac{1}{2} \sqrt{\frac{\sum_{k=1}^K k^2 \lambda_k}{\sum_{k=1}^K w_k}} \quad (8)$$

$$\geq \frac{1}{2} \sqrt{\frac{\left(\prod_{k=1}^K k^2 \lambda_k\right)^{1/K} K}{\sum_{k=1}^K w_k}} \quad (9)$$

$$= \frac{1}{2} \sqrt{\frac{(K!)^{2/K} |\mathbf{H}|^{1/K} K}{\sum_{k=1}^K w_k}} \quad (10)$$

where (9) results from the arithmetic-geometric mean inequality, and (10) from the determinant of \mathbf{H} being equal to the product of its eigenvalues. Note that the bounding function in (10) does not depend on the ordering of the eigenvalues. Moreover, since

$$|\mathbf{H}| = \prod_{k=1}^K \Phi_{kk}^2$$

where Φ is defined via the Cholesky factorization $\mathbf{H} = \Phi^T \Phi$, we now use the fact that for the ZF-DFR, the QoS constraints are satisfied whenever $\Phi_{kk}^2 \geq \eta_k w_k$. Hence, we find that the time-bandwidth product of any signal set that satisfies the SIR constraints for the ZF-DFR is lower-bounded as

$$BT \geq \frac{1}{2} \max \left\{ 1, \sqrt{\frac{(K!)^{2/K} \left(\prod_{k=1}^K \eta_k w_k\right)^{1/K} K}{\sum_{k=1}^K w_k}} \right\}. \quad (11)$$

Unlike the OOMA upper bound, this bound is in general unachievable because it is not clear that there exist positive semidefinite matrices \mathbf{H} whose eigenvalues and diagonal elements of the Cholesky factor Φ can be chosen independently to satisfy the inequalities in (9) and (11) with equality. Even if they did, it is not clear how one would actually construct such matrices.

In the remainder of the paper, we will develop a constructive signal design procedure for the three DFRs, which in the case of the ZF-DFR will be shown, in the numerical examples

of Section V, to yield a bandwidth that is quite close to the unachievable lower bound in (11). This would not only imply that the bound in (11) is tight but also that our signal design algorithm can yield signals with nearly minimum bandwidth.

2) *The Design Strategy:* Our goal is to find signal sets that require a bandwidth that is much lower than that needed for OOMA. Our strategy is to construct a good correlation matrix \mathbf{H} in a recursive fashion. Once \mathbf{H} is obtained, the signals are determined to minimize bandwidth as follows: obtain the spectral decomposition $\mathbf{H} = \mathbf{V}\mathbf{\Lambda}\mathbf{V}^T$ with the eigenvalues in $\mathbf{\Lambda}$ arranged in nonincreasing order and construct the vector of transmitter pulses $\mathbf{s}(t) = [s_1(t), \dots, s_K(t)]^T$ as $\mathbf{V}\mathbf{\Lambda}^{1/2}\mathbf{\Phi}(t)$ where the vector of orthonormal basis functions $\mathbf{\Phi}(t)$ consists of the minimum rms bandwidth sinusoidal pulses in the case of rms bandwidth (cf. [3]) the time-truncated prolate spheroidal wave functions (cf. [6]) in the case of FOBP bandwidth, or the minimum fourth-moment bandwidth basis functions for the fourth-moment bandwidth [12].

The rest of this paper deals with the problem of constructing the correlation matrix. We start by observing that if there is no error propagation, the SIR performance of a particular user for any DFR with $\mathbf{B} = \mathcal{L}(\mathbf{FR})$ is independent of the correlations between that user and the users with lower indices. This fact suggests a recursive construction of \mathbf{H} where the correlations are specified between signals in the reverse order in which the users are decoded. The idea is to start with the last two users' signals and determine their correlation matrix so that the given DFR just achieves the specified SIR for the second-to-last user. With the correlation matrix of the last two users' signals fixed, we then determine how the third-to-last user's signal is to be correlated with them so that the SIR of this user just meets the SIR constraint. This process continues so that for the k th user we add a top row, $\underline{\mathbf{H}}_{(k)}^T$ (and a left column, $\underline{\mathbf{H}}_{(k)}$) to $\mathbf{H}_{(k+1)}$ to obtain $\mathbf{H}_{(k)}$. At each step, there are infinitely many such augmentations that will meet the target SIR constraint for the k th user without altering the SIRs for users $K, K-1, \dots, k+1$. Out of these, we propose to choose the matrix that makes the bandwidth of the superposition of signals from users k, \dots, K as small as possible at each step. Though not optimal, such a greedy algorithm will be shown to yield good results and finds justification in the interlacing property of the eigenvalues of a matrix and its principal submatrix. In particular, let $B_{(k)}$ denote the bandwidth required by $\mathbf{H}_{(k)}$ and let $\zeta = w_k(\sum_{i=k+1}^K w_i)^{-1}$. Then from (3) and the interlacing-eigenvalue theorem [15], it can be shown that

$$(2TB_{(k)})^2 \geq \frac{\zeta + (2TB_{(k+1)})^2}{\zeta + 1}. \quad (12)$$

While not a strict analytical justification for our heuristic, the above inequality gives an intuitive idea of why it would work. Note that $B_{(k)}$ is bounded from below by a function that is monotonically increasing in $B_{(k+1)}$. Thus a poor choice for $\mathbf{H}_{(k+1)}$ will yield a larger value for $B_{(k+1)}$ than necessary and increase the lower bound on $B_{(k)}$.

As we recursively design \mathbf{H} , we must guarantee that the final matrix is positive semidefinite else it would not be a valid correlation matrix. Thus given a positive semidefinite $\mathbf{H}_{(k+1)}$, not

every choice for $\underline{\mathbf{H}}_{(k)}$ is valid. Necessary and sufficient conditions for $\underline{\mathbf{H}}_{(k)}$ to satisfy the positive semidefinite (PSD) constraint are given [1, Lemma 3]. In fact, in that paper, a convenient reparameterization of the problem was given which we state next.

Let the spectral decomposition of $\mathbf{H}_{(k+1)}$ be given by

$$\mathbf{H}_{(k+1)} = \mathbf{V}\mathbf{L}\mathbf{V}^T \quad (13)$$

where \mathbf{L} is an invertible diagonal matrix. If the rank of $\mathbf{H}_{(k+1)}$ is $M \leq K - k$, then \mathbf{V} is $K - k \times M$ and \mathbf{L} is $M \times M$. We denote the m th column of \mathbf{V} by $\underline{\mathbf{V}}_m$ so that $\mathbf{V} = [\underline{\mathbf{V}}_1 \dots \underline{\mathbf{V}}_M]$. The diagonal elements of \mathbf{L} , (l_1, l_2, \dots, l_M) , are the nonzero eigenvalues of $\mathbf{H}_{(k+1)}$, and they are ordered so that $l_1 \geq l_2 \geq \dots \geq l_M$. It was shown in [1] that a necessary and sufficient condition for $\mathbf{H}_{(k)}$ to be a PSD matrix is the following PSD constraint:

$$\underline{\mathbf{H}}_{(k)} \in \{\mathbf{V}\underline{\mathbf{D}}: \underline{\mathbf{D}}^T\mathbf{L}^{-1}\underline{\mathbf{D}} \leq w_k\}. \quad (14)$$

The SIR constraints for the DFRs of interest, as given in (5) and (6) in terms of $\underline{\mathbf{H}}_{(k)}$, can be reparameterized in terms of $\underline{\mathbf{D}}$ as follows:

CM-DFR:

$$\underline{\mathbf{H}}_{(k)} \in \{\mathbf{V}\underline{\mathbf{D}}: \underline{\mathbf{D}}^T(\mathbf{L} + \sigma^2\mathbf{I})^{-1}\underline{\mathbf{D}} \leq w_k(1 - \eta_k)\} \quad (15)$$

ZF-DFR:

$$\underline{\mathbf{H}}_{(k)} \in \{\mathbf{V}\underline{\mathbf{D}}: \underline{\mathbf{D}}^T\mathbf{L}^{-1}\underline{\mathbf{D}} \leq w_k(1 - \eta_k)\} \quad (16)$$

Suc. Cancel:

$$\underline{\mathbf{H}}_{(k)} \in \left\{ \mathbf{V}\underline{\mathbf{D}}: \underline{\mathbf{D}}^T(\sigma^2\mathbf{I})^{-1}\underline{\mathbf{D}} \leq \frac{w_k}{\eta_k}(1 - \eta_k) \right\}. \quad (17)$$

It is clear that if $\eta_k = 1$, then only $\underline{\mathbf{H}}_{(k)} = \mathbf{V}\underline{\mathbf{D}} = \mathbf{0}$ will work. Otherwise, we know that $\eta_k \in (0, 1)$, and this implies that

$$w_k(1 - \eta_k) \in (0, w_k) \quad (18)$$

$$\frac{w_k}{\eta_k}(1 - \eta_k) \in (0, \infty). \quad (19)$$

The PSD constraint in (14) along with one of the SIR constraints from (15)–(17) form the two ellipsoidal constraint sets to which $\underline{\mathbf{D}}$ must belong. The problem is to choose $\underline{\mathbf{D}}$ lying within their intersection that minimizes the bandwidth required for $\mathbf{H}_{(k)}$. Note that the reparameterization in terms of $\underline{\mathbf{D}}$ is particularly convenient since these ellipsoids not only share the same set of orthogonal axes $\{\underline{\mathbf{V}}_i\}_{i=1}^M$ but they also have the same orientation since the diagonal elements of \mathbf{L} , $\mathbf{L} + \sigma^2\mathbf{I}$, and $\sigma^2\mathbf{I}$ are all arranged in the nonincreasing order.

III. AN ANALYSIS OF THE CONSTRAINT SETS

In this section, we develop certain analytical results that give us some insight about good (though not the best) choices for $\underline{\mathbf{D}}$ within the intersection of the PSD and SIR constraint sets.

Unlike the PSD and SIR constraints, the bandwidth does not lend itself to an analytical representation in terms of $\underline{\mathbf{D}}$. Hence, obtaining a $\underline{\mathbf{D}}$ that minimizes the bandwidth subject to the constraints appears to be intractable. However, the rms bandwidth associated with a weighted correlation matrix is proportional to a weighted sum of its eigenvalues, where the weighting of the k th-largest eigenvalue is k^2 . Since the largest eigenvalue of $\mathbf{H}_{(k)}$ has the smallest weighting coefficient, we consider a maximization of the largest eigenvalue of $\mathbf{H}_{(k)}$ over $\underline{\mathbf{D}}$. Similarly, suppose that the rank of $\mathbf{H}_{(k+1)}$ is M , then the rank of $\mathbf{H}_{(k)}$

will be either M or $M + 1$. Thus the $(M + 1)$ th-largest eigenvalue of $\mathbf{H}_{(k)}$ is the smallest potentially nonzero eigenvalue and its weighting coefficient in the rms bandwidth formula is hence the highest. For this reason, we will also consider minimizing this eigenvalue over \underline{D} .

A. Maximizing the Largest Eigenvalue of $\mathbf{H}_{(k)}$

The following lemma is applicable to both SIR and PSD constraints. It is key in regard to our investigation of the eigenvalues.

Lemma 2: Given PSD matrices \mathbf{C} (with pseudo-inverse \mathbf{C}^+) and $\mathbf{H}_{(k+1)}$, with the latter admitting a singular-value decomposition (SVD) $\mathbf{H}_{(k+1)} = \mathbf{V}\mathbf{L}\mathbf{V}^T$, and given vector \underline{z} , scalar y , and positive scalars w_k and α , we have

$$\begin{aligned} f(y, \underline{z}) &\triangleq \max_{\{\underline{D}: \underline{D}^T \mathbf{C}^+ \underline{D} \leq \alpha\}} [y \quad \underline{z}^T] \begin{bmatrix} w_k & \underline{D}^T \mathbf{V}^T \\ \mathbf{V} \underline{D} & \mathbf{H}_{(k+1)} \end{bmatrix} \begin{bmatrix} y \\ \underline{z} \end{bmatrix} \\ &= w_k y^2 + \underline{z}^T \mathbf{H}_{(k+1)} \underline{z} + 2|y| \sqrt{\alpha} \sqrt{\underline{z}^T \mathbf{V} \mathbf{C} \mathbf{V}^T \underline{z}} \end{aligned} \quad (20)$$

and

$$\begin{aligned} g(y, \underline{z}) &\triangleq \min_{\{\underline{D}: \underline{D}^T \mathbf{C}^+ \underline{D} \leq \alpha\}} [y \quad \underline{z}^T] \begin{bmatrix} w_k & \underline{D}^T \mathbf{V}^T \\ \mathbf{V} \underline{D} & \mathbf{H}_{(k+1)} \end{bmatrix} \begin{bmatrix} y \\ \underline{z} \end{bmatrix} \\ &= w_k y^2 + \underline{z}^T \mathbf{H}_{(k+1)} \underline{z} - 2|y| \sqrt{\alpha} \sqrt{\underline{z}^T \mathbf{V} \mathbf{C} \mathbf{V}^T \underline{z}}. \end{aligned} \quad (21)$$

The set of arguments which yield the maximum is

$$\left\{ \underline{D}: \mathbf{C}^+ \underline{D} = \frac{y}{|y|} \sqrt{\frac{\alpha}{\underline{z}^T \mathbf{V} \mathbf{C} \mathbf{V}^T \underline{z}}} \mathbf{V}^T \underline{z} \right\} \quad (22)$$

and the set of arguments which yield the minimum is

$$\left\{ \underline{D}: \mathbf{C}^+ \underline{D} = \frac{-y}{|y|} \sqrt{\frac{\alpha}{\underline{z}^T \mathbf{V} \mathbf{C} \mathbf{V}^T \underline{z}}} \mathbf{V}^T \underline{z} \right\}. \quad (23)$$

Proof: Letting $\alpha' \in [0, \alpha]$ be arbitrary, we work with the constraint that $\underline{D}^T \mathbf{C}^+ \underline{D} = \alpha'$. Defining the Lagrangian as

$$f(\underline{D}, \delta) = w_k y^2 + 2y \underline{D}^T \mathbf{V}^T \underline{z} + \underline{z}^T \mathbf{H}_{(k+1)} \underline{z} + \delta(\alpha' - \underline{D}^T \mathbf{C}^+ \underline{D}) \quad (24)$$

and setting $\partial f / \partial \underline{D}$ equal to zero yields

$$\mathbf{C}^+ \underline{D} = \delta^{-1} y \mathbf{V}^T \underline{z}. \quad (25)$$

Noting the property of the pseudo-inverse that $\mathbf{C}^+ = \mathbf{C}^+ \mathbf{C} \mathbf{C}^+$, we find that δ must be chosen so that

$$\delta^{-2} y^2 \underline{z}^T \mathbf{V} \mathbf{C} \mathbf{V}^T \underline{z} = \alpha'.$$

Thus

$$\delta = \pm \frac{|y|}{\sqrt{\alpha'}} \sqrt{\underline{z}^T \mathbf{V} \mathbf{C} \mathbf{V}^T \underline{z}} \quad (26)$$

where the positive choice maximizes $f(\underline{D}, \delta)$, since it becomes a concave function, and the negative choice minimizes it, since

the function becomes convex. Considering only the maximization of f , we choose the former and denote it by δ_o . Using (25) and (26) we find that

$$2y \underline{D}^T \mathbf{V}^T \underline{z} = 2\delta_o \underline{D}^T \mathbf{C}^+ \underline{D} \quad (27)$$

$$= 2\delta_o \alpha' \quad (28)$$

$$= 2|y| \sqrt{\alpha'} \sqrt{\underline{z}^T \mathbf{V} \mathbf{C} \mathbf{V}^T \underline{z}}. \quad (29)$$

This is increasing in α' so the optimum $\alpha' = \alpha$. It only remains to substitute (29) into the quadratic objective function that was to be maximized. The minimization is accomplished by choosing the minimizing value of δ and proceeding similarly. \square

The matrix \mathbf{C} in the above lemma can represent any one of the constraining matrices in (14) or (15)–(17) whereas α represents $w_k(1 - \eta_k)$ for both the CM-DFR and ZF-DFR, $\frac{w_k}{\eta_k}(1 - \eta_k)$ for successive cancellation, and w_k for the PSD constraint. The following theorem obtains the $\underline{H}_{(k)}$ that maximizes the largest eigenvalue of $\mathbf{H}_{(k)}$ subject to one of these constraints.

Theorem 1: With the hypotheses of Lemma 2, let $\lambda(\underline{D})$ denote the maximum eigenvalue of $\mathbf{H}_{(k)}$ given that $\underline{H}_{(k)} = \mathbf{V} \underline{D}$. Then

$$\max_{\{\underline{D}: \underline{D}^T \mathbf{C}^+ \underline{D} \leq \alpha\}} \lambda(\underline{D}) = l_1 + \frac{w_k - l_1}{X} \left(X y_o^2 + 2y_o \sqrt{1 - y_o^2} \right) \quad (30)$$

where $y_o = \sqrt{2}(4 + X^2 - X\sqrt{4 + X^2})^{-1/2}$ and

$$X = \begin{cases} (w_k - l_1) / \sqrt{\alpha(l_1 + \sigma^2)}, & \text{if } \mathbf{C} = \mathbf{L} + \sigma^2 \mathbf{I}, \text{ CM-DFR} \\ (w_k - l_1) / \sqrt{\alpha l_1}, & \text{if } \mathbf{C} = \mathbf{L}, \text{ ZF-DFR and PSD constraint} \\ (w_k - l_1) / \sqrt{\alpha \sigma^2}, & \text{if } \mathbf{C} = \sigma^2 \mathbf{I}, \text{ Suc. Cancel.} \end{cases} \quad (31)$$

The corresponding assignment for $\underline{H}_{(k)}$ is

$$\underline{H}_{(k)} = \begin{cases} \sqrt{\alpha(l_1 + \sigma^2)} \underline{V}_1, & \text{CM-DFR} \\ \sqrt{\alpha l_1} \underline{V}_1, & \text{ZF-DFR and PSD constraint} \\ \sqrt{\alpha \sigma^2} \underline{V}_1, & \text{Suc. Cancel.} \end{cases} \quad (32)$$

Proof: We prove the theorem for the CM-DFR. The proofs for the other receivers are similar. Choosing \underline{D} as in (22), we seek to maximize the function $f(y, \underline{z})$ in (20) over the set of y, \underline{z} such that $y^2 + \underline{z}^T \underline{z} = 1$. The resulting maximum value of $f(y, \underline{z})$ is, according to the Rayleigh–Ritz theorem [15], the maximum eigenvalue of $\mathbf{H}_{(k)}$. Substituting $\mathbf{C} = \mathbf{L} + \sigma^2 \mathbf{I}$ into (20) and using the SVD in (13), we have

$$f(y, \underline{z}) = w_k y^2 + \underline{z}^T \mathbf{H}_{(k+1)} \underline{z} + 2|y| \sqrt{\alpha} \cdot \sqrt{\underline{z}^T \mathbf{H}_{(k+1)} \underline{z} + \sigma^2 \underline{z}^T \mathbf{V} \mathbf{V}^T \underline{z}}. \quad (33)$$

Since $f(y, \underline{z})$ is an even function of y , we can assume without loss of generality that $y \in [0, 1]$. For a given y , we maximize $f(y, \underline{z})$ over the set of \underline{z} such that $\underline{z}^T \underline{z} = 1 - y^2$. $f(y, \underline{z})$ depends on \underline{z} through the two quadratic terms $\underline{z}^T \mathbf{H}_{(k+1)} \underline{z}$ and $\underline{z}^T \mathbf{V} \mathbf{V}^T \underline{z}$ and is monotonically increasing in both those terms. Fortunately, the two terms are simultaneously maximized by the same \underline{z} . Using the Rayleigh–Ritz theorem again, the maximum of $\underline{z}^T \mathbf{H}_{(k+1)} \underline{z}$ subject to $\underline{z}^T \underline{z} = 1 - y^2$ occurs when \underline{z} is proportional to the eigenvector corresponding to the largest eigenvalue of $\mathbf{H}_{(k+1)}$. Specifically, $\underline{z} = \sqrt{1 - y^2} \underline{V}_1$ where \underline{V}_1 is

the first column vector of \mathbf{V} . Let us now consider the maximization of $\underline{\mathbf{Z}}^T \mathbf{V} \mathbf{V}^T \underline{\mathbf{Z}}$. Define $\underline{\mathbf{V}}$ so that $[\mathbf{V} \ \underline{\mathbf{V}}]$ is a $K - k \times K - k$ orthogonal matrix. We have

$$1 - y^2 = \underline{\mathbf{Z}}^T \underline{\mathbf{Z}} \quad (34)$$

$$= \underline{\mathbf{Z}}^T [\mathbf{V} \ \underline{\mathbf{V}}] [\mathbf{V} \ \underline{\mathbf{V}}]^T \underline{\mathbf{Z}} \quad (35)$$

$$\geq \underline{\mathbf{Z}}^T \mathbf{V} \mathbf{V}^T \underline{\mathbf{Z}}. \quad (36)$$

In particular, for $\underline{\mathbf{Z}} = \sqrt{1 - y^2} \underline{\mathbf{V}}_1$, the upper bound on $\underline{\mathbf{Z}}^T \mathbf{V} \mathbf{V}^T \underline{\mathbf{Z}}$ is met with equality. Hence, $\underline{\mathbf{Z}} = \sqrt{1 - y^2} \underline{\mathbf{V}}_1$ maximizes $f(y, \underline{\mathbf{Z}})$ for a given y . Denoting this maximum as $f(y)$, we have

$$f(y) = y^2(w_k - l_1) + l_1 + 2\sqrt{\alpha(l_1 + \sigma^2)}y\sqrt{1 - y^2}. \quad (37)$$

Taking the derivative of f with respect to y and setting the result equal to zero we find that

$$(w_k - l_1)y + \sqrt{\alpha(l_1 + \sigma^2)} \frac{1 - 2y^2}{\sqrt{1 - y^2}} = 0 \quad (38)$$

for $y \in [0, 1)$. We use the substitution

$$X = (w_k - l_1) / \sqrt{\alpha(l_1 + \sigma^2)}$$

and some algebraic manipulation to see that

$$y = \begin{cases} -\frac{1 - 2y^2}{X\sqrt{1 - y^2}}, & \text{if } X \neq 0 \\ \sqrt{\frac{1}{2}}, & \text{if } X = 0. \end{cases} \quad (39)$$

Squaring both sides and rearranging terms yields an equation that is quadratic in y^2

$$y^4(4 + X^2) + y^2(-4 - X^2) + 1 = 0. \quad (40)$$

Hence

$$y^2 = \frac{1}{2} \left(1 \pm \frac{X}{\sqrt{4 + X^2}} \right). \quad (41)$$

Note that the right-hand side is an element of $(0, 1)$ since if $X \geq 0$ then $\frac{X}{\sqrt{4 + X^2}} \in [0, 1)$ and if $X < 0$ then $\frac{X}{\sqrt{4 + X^2}} \in (-1, 0)$. Thus $y \in (0, 1)$ and so (38) is valid. The two possibilities for y^2 in (41) can be substituted into (39) to yield

$$y_i = -\frac{(1 - 2K_i)}{X\sqrt{1 - K_i}}, \quad \text{for } i = 1, 2 \quad (42)$$

where we define

$$K_1 = \frac{1}{2} \left(1 + \frac{X}{\sqrt{4 + X^2}} \right)$$

and

$$K_2 = \frac{1}{2} \left(1 - \frac{X}{\sqrt{4 + X^2}} \right).$$

It is easy to check that $y_1 \geq 0$ and $y_2 \leq 0$ for all X . Since in this proof we have required y to be nonnegative, there is a *unique* value for y , which we call y_o , for which the derivative of $f(y)$ is zero, namely,

$$y_o = \begin{cases} y_1, & \text{if } X < 0 \\ \sqrt{\frac{1}{2}}, & \text{if } X = 0 \\ y_1, & \text{if } X > 0 \end{cases} \quad (43)$$

$$= \sqrt{2} \left(4 + X^2 - X\sqrt{4 + X^2} \right)^{-1/2}, \quad \text{for all } X. \quad (44)$$

As a check it is easy to see that as X goes to negative infinity, y_o goes to zero, and with a little work we find that as X goes to positive infinity, y_o goes to unity. Also, to see that $f(y_o)$ corresponds to the maximum value over $y \in [0, 1]$, one can explicitly

calculate the second derivative of $f(y)$ at $y = y_o$ and find that it is negative.

Finally, we must compute the $\underline{\mathbf{H}}_{(k)}$ that yields the maximum. Using the result from this proof that $\underline{\mathbf{Z}} = \sqrt{1 - y_o^2} \underline{\mathbf{V}}_1$, we obtain the following equalities starting from (22):

$$\mathbf{C}^+ \underline{\mathbf{D}} = \frac{y}{|y|} \sqrt{\frac{\alpha}{\underline{\mathbf{Z}}^T \mathbf{V} \mathbf{C} \mathbf{V}^T \underline{\mathbf{Z}}}} \mathbf{V}^T \underline{\mathbf{Z}} \quad (45)$$

$$(\mathbf{L} + \sigma^2 \mathbf{I})^{-1} \underline{\mathbf{D}} = \sqrt{\frac{\alpha}{(1 - y_o^2)(l_1 + \sigma^2)}} \sqrt{1 - y_o^2} \mathbf{V}^T \underline{\mathbf{V}}_1 \quad (46)$$

$$\mathbf{V} \underline{\mathbf{D}} = \sqrt{\frac{\alpha}{l_1 + \sigma^2}} \mathbf{V} (\mathbf{L} + \sigma^2 \mathbf{I}) \mathbf{V}^T \underline{\mathbf{V}}_1 \quad (47)$$

$$\underline{\mathbf{H}}_{(k)} = \sqrt{\alpha(l_1 + \sigma^2)} \underline{\mathbf{V}}_1. \quad (48)$$

□

B. Minimizing the Smallest Potentially Nonzero Eigenvalue of $\underline{\mathbf{H}}_{(k)}$

In this section, we consider the problem of minimizing the smallest potentially nonzero eigenvalue of $\underline{\mathbf{H}}_{(k)}$ subject to an ellipsoidal constraint. This is also the $(M + 1)$ th-largest eigenvalue of $\underline{\mathbf{H}}_{(k)}$ because, given that the rank of $\underline{\mathbf{H}}_{(k+1)}$ is M , the rank of $\underline{\mathbf{H}}_{(k)}$ can be no greater than $M + 1$. Minimizing the $(M + 1)$ th-largest eigenvalue transfers power away from this eigenvalue which is desirable, because among all the nonzero eigenvalues, this particular eigenvalue has the largest scale factor in the expression for minimum bandwidth as indicated by (3). Consider the next theorem.

Theorem 2: With the hypotheses of Lemma 2, let $\lambda(\underline{\mathbf{D}})$ denote the $(M + 1)$ th-largest eigenvalue of $\underline{\mathbf{H}}_{(k)}$ given that $\underline{\mathbf{H}}_{(k)} = \mathbf{V} \underline{\mathbf{D}}$. We have

$$\min_{\{\underline{\mathbf{D}}: \underline{\mathbf{D}}^T \mathbf{C}^+ \underline{\mathbf{D}} \leq \alpha\}} \lambda(\underline{\mathbf{D}}) = l_M + \frac{w_k - l_M}{X} \left(X y_o^2 - 2 y_o \sqrt{1 - y_o^2} \right) \quad (49)$$

where $y_o = \sqrt{2} (4 + X^2 + X\sqrt{4 + X^2})^{-1/2}$ and

$$X = \begin{cases} (w_k - l_M) / \sqrt{\alpha(l_M + \sigma^2)}, & \text{if } \mathbf{C} = \mathbf{L} + \sigma^2 \mathbf{I}, \text{ CM-DFR} \\ (w_k - l_M) / \sqrt{\alpha l_M}, & \text{if } \mathbf{C} = \mathbf{L}, \text{ ZF-DFR and PSD constraint} \\ (w_k - l_M) / \sqrt{\alpha \sigma^2}, & \text{if } \mathbf{C} = \sigma^2 \mathbf{I}, \text{ Suc. Cancel.} \end{cases} \quad (50)$$

The corresponding assignment for $\underline{\mathbf{H}}_{(k)}$ is

$$\underline{\mathbf{H}}_{(k)} = \begin{cases} \sqrt{\alpha(l_M + \sigma^2)} \underline{\mathbf{V}}_M, & \text{CM-DFR} \\ \sqrt{\alpha l_M} \underline{\mathbf{V}}_M, & \text{ZF-DFR and PSD Constraint.} \\ \sqrt{\alpha \sigma^2} \underline{\mathbf{V}}_M, & \text{Suc. Cancel.} \end{cases} \quad (51)$$

The proof of Theorem 2 is long and has several subtleties. It is outlined in the Appendix.

C. On the Intersection of the PSD and SIR Ellipsoids

We return to the constraint sets defined by (14) and one of (15)–(17). In normalized form, the PSD and SIR constraints can be expressed as

$$\sum_{j=1}^M d_j^2 (l_j \alpha_{\text{psd}})^{-1} \leq 1 \quad (52)$$

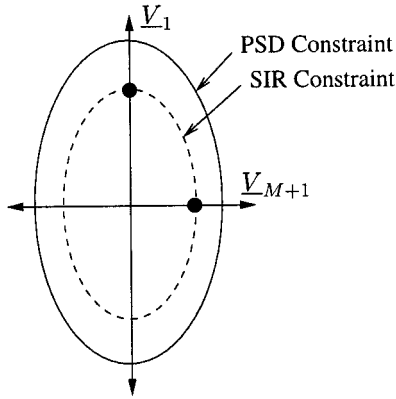


Fig. 2. Category 1: The SIR constraint subsumes the PSD constraint. Two points are considered, at the intersection of axes \underline{V}_1 and \underline{V}_{M+1} with boundary of the SIR ellipsoid.

and

$$\text{CM-DFR: } \sum_{j=1}^M d_j^2 ((l_j + \sigma^2) \alpha_{\text{cm}})^{-1} \leq 1 \quad (53)$$

$$\text{ZF-DFR: } \sum_{j=1}^M d_j^2 (l_j \alpha_{\text{zf}})^{-1} \leq 1 \quad (54)$$

$$\text{Suc. Cancel.: } \sum_{j=1}^M d_j^2 (\sigma^2 \alpha_{\text{sc}})^{-1} \leq 1 \quad (55)$$

where

$$\alpha_{\text{psd}} = w_k, \quad \alpha_{\text{cm}} = \alpha_{\text{zf}} = w_k(1 - \eta_k) \leq \alpha_{\text{psd}},$$

$$\text{and } \alpha_{\text{sc}} = \frac{w_k}{\eta_k}(1 - \eta_k). \quad (56)$$

The following lemma from [1] tells us something about the intersection of the two constraint sets.

Lemma 3: For $1 \leq j \leq M$ we define x_j for the three receiver types

$$x_j = \begin{cases} (l_j \alpha_{\text{psd}})^{-1} - ((l_j + \sigma^2) \alpha_{\text{cm}})^{-1} & \text{CM-DFR} \\ (l_j \alpha_{\text{psd}})^{-1} - (l_j \alpha_{\text{zf}})^{-1} & \text{ZF-DFR} \\ (l_j \alpha_{\text{psd}})^{-1} - (\sigma^2 \alpha_{\text{sc}})^{-1} & \text{Suc. Cancel.} \end{cases} \quad (57)$$

Then we have that $x_j \leq 0$ implies that $x_{j-1} \leq 0$, and $x_j \geq 0$ implies that $x_{j+1} \geq 0$, and $x_j < 0$ implies that $x_{j-1} < 0$, and $x_j > 0$, implies that $x_{j+1} > 0$.

This lemma implies that there exists a $\tilde{j} \in \{1, \dots, M\}$ such that $x_j \leq 0$ for all $j \leq \tilde{j}$ and $x_j \geq 0$ for all $j \geq \tilde{j}$. The SIR constraint is at least as restrictive along the axes 1 through \tilde{j} , while the PSD constraint is at least as restrictive along the axes \tilde{j} through M . Note that if $\tilde{j} = M$, then the ellipsoid of the SIR constraint lies inside the ellipsoid of the PSD constraint. The ZF-DFR is special in this sense because the SIR constraint always subsumes the PSD constraint. If instead $\tilde{j} = 1$, then the ellipsoid of the PSD constraint lies within the ellipsoid of the SIR constraint. Finally, if $1 < \tilde{j} < M$, then neither of the ellipsoids lies wholly within the other.

When the SIR constraint subsumes the PSD constraint (Category 1) or vice versa (Category 2), good signal-design methods can be based on the results of Theorems 1 and 2 as described in the next section. When the intersection of the ellipsoids is

nontrivial (Category 3), we are interested in analytically finding points that lie on the boundary of their intersection. The set of intersection points is rather complex, so we will consider only those points of intersection that lie in one of the two-dimensional *slices* formed by the major axis \underline{V}_1 and one of the other axes. That is, for any $j > 1$, we consider the intersection of the $\underline{V}_1 - \underline{V}_j$ plane with the two ellipsoids of interest. After taking one of these slices, the two constraints are representable by two two-dimensional ellipses. To this end, suppose that $x_1 < 0$ and $x_M \geq 0$, then let $j' = \min\{j: x_j \geq 0\}$ so that $x_j \geq 0$ when $j' \leq j \leq M$ by Lemma 3. For any $j \geq j'$ we make a slice defined by the axes \underline{V}_1 and \underline{V}_j . That is, set $d_i = 0$ for all i not equal to 1 or j . Since $x_1 < 0$ and $x_j \geq 0$, we are guaranteed that the boundaries of these two ellipses intersect. The points where their boundaries intersect are given by $(\pm|d'_1|, \pm|d'_j|)$, where

$$(d'_1)^2 = \begin{cases} \left(\frac{l_1(l_1 + \sigma^2)}{\sigma^2} \right) & \\ \frac{\alpha_{\text{cm}}(l_j + \sigma^2) - \alpha_{\text{psd}} l_j}{l_1 - l_j} & \text{CM-DFR} \\ l_1 \frac{\alpha_{\text{sc}} \sigma^2 - \alpha_{\text{psd}} l_j}{l_1 - l_j} & \text{Suc. Cancel.} \end{cases} \quad (58)$$

$$(d'_j)^2 = \begin{cases} \left(\frac{l_j(l_j + \sigma^2)}{\sigma^2} \right) & \\ \frac{-\alpha_{\text{cm}}(l_1 + \sigma^2) + \alpha_{\text{psd}} l_1}{l_1 - l_j} & \text{CM-DFR} \\ l_j \frac{-\alpha_{\text{sc}} \sigma^2 + \alpha_{\text{psd}} l_1}{l_1 - l_j} & \text{Suc. Cancel.} \end{cases} \quad (59)$$

The next lemma is used to decide on the preferred slice. Its importance will become apparent in Section IV when considering signal design for Category 3.

Lemma 4: Over the set of j such that $j \geq j'$, $(d'_1)^2$ as given in (58) is maximized for $j = M$.

Proof: Considering only the CM-DFR, we have that the partial derivative of $(\alpha_{\text{cm}}(l_j + \sigma^2) - \alpha_{\text{psd}} l_j) / (l_1 - l_j)$ with respect to l_j is equal to a positive constant times $\alpha_{\text{cm}}(l_1 + \sigma^2) - \alpha_{\text{psd}} l_1$. The fact that $x_1 < 0$ thus implies that $(d'_1)^2$ is decreasing in l_j . Choosing $j = M$ minimizes l_j and, therefore, maximizes $(d'_1)^2$. \square

We now have the tools necessary to give a general method for designing signal sets that allow the users to achieve the SIR specifications in a bandwidth-efficient manner.

IV. SIGNAL DESIGN FOR BEMA

In general, there is a nondenumerable set of $\underline{H}_{(k)}$ that lie within the intersection of the two ellipsoidal constraint sets. Because this intersection becomes rather unwieldy for larger dimensions, it is desirable to avoid anything resembling an exhaustive search of the region. In the following, we present a simple and general design methodology that finds rigorous justification based on the analytical results of the previous section.

We partition the set of constraints into three categories and then use the results of Section III to choose $\underline{H}_{(k)}$ appropriately within each category.

Category 1: The SIR constraint subsumes the PSD constraint. Lemma 3 implies $x_M < 0$, and hence that $x_j < 0$ for all j . See Fig. 2 for a two-dimensional example. From the PSD constraint in (14) and the SIR constraint in (15)–(17), it is clear that for the CM-DFR or successive cancellation the constraint

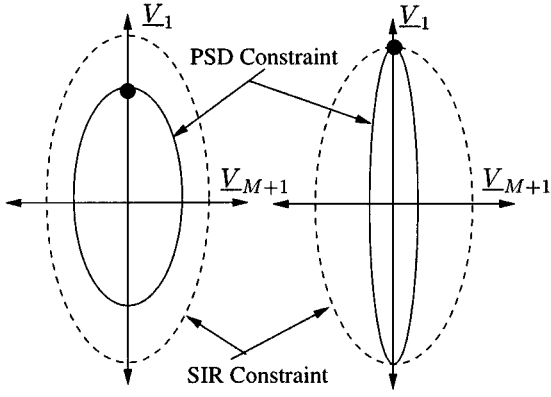


Fig. 3. The two possibilities of Category 2. The chosen point lies on the intersection of axis \underline{V}_1 and the boundary of the PSD ellipsoid.

sets will fall into this category for large enough η_k , while for the ZF-DFR the constraint sets always fall into this category.

We consider two choices and settle with the one that yields a smaller bandwidth for $\mathbf{H}_{(k)}$. The first choice is motivated by Theorem 1 and maximizes the largest eigenvalue of $\mathbf{H}_{(k)}$ subject to the SIR constraint, i.e.,

$$\underline{\mathbf{H}}_{(k)} = \begin{cases} \sqrt{w_k(1-\eta_k)(l_1 + \sigma^2)}\underline{V}_1 & \text{CM-DFR} \\ \sqrt{w_k(1-\eta_k)l_1}\underline{V}_1 & \text{ZF-DFR} \\ \sqrt{\frac{w_k}{\eta_k}(1-\eta_k)\sigma^2}\underline{V}_1 & \text{Suc. Cancel.} \end{cases} \quad (60)$$

The second choice is based on Theorem 2 and minimizes the $(M+1)$ th eigenvalue of $\mathbf{H}_{(k)}$, i.e.,

$$\underline{\mathbf{H}}_{(k)} = \begin{cases} \sqrt{w_k(1-\eta_k)(l_M + \sigma^2)}\underline{V}_M & \text{CM-DFR} \\ \sqrt{w_k(1-\eta_k)}\underline{V}_M & \text{ZF-DFR} \\ \sqrt{\frac{w_k}{\eta_k}(1-\eta_k)\sigma^2}\underline{V}_M & \text{Suc. Cancel.} \end{cases} \quad (61)$$

Category 2: The PSD constraint is at least as restrictive as the SIR constraint along the major axis \underline{V}_1 . Lemma 3 implies that $x_1 \geq 0$, and hence that $x_j \geq 0$ for all j . See Fig. 3 for a two-dimensional example. The PSD constraint in (14) and the SIR constraint in (15)–(17) imply that for the CM-DFR and successive cancellation the constraint sets fall into Category 2 whenever η_k is small enough, and that the ZF-DFR constraint sets never fall into this category.

For Category 2, we let

$$\underline{\mathbf{H}}_{(k)} = \sqrt{w_k l_1}\underline{V}_1 \quad (62)$$

for this maximizes the largest eigenvalue, as indicated by Theorem 1, while simultaneously setting the $(M+1)$ th-largest eigenvalue to zero. The latter follows since any point that lies on the boundary of the PSD constraint causes the $(M+1)$ th-largest eigenvalue to be zero.

Category 3: Neither the SIR nor the PSD constraint is dominant. Lemma 3 implies that $x_1 < 0$ and $x_M \geq 0$. See Fig. 4 for a two-dimensional example.

In Category 3, we again consider two possible choices for $\underline{\mathbf{H}}_{(k)}$, choosing the one that requires lesser bandwidth for $\mathbf{H}_{(k)}$. The first results from the fact that the SIR constraint is more

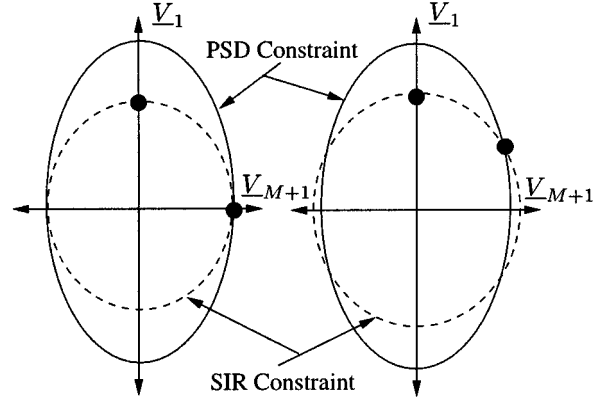


Fig. 4. The two possibilities of Category 3 for the two-dimensional case. One of two points is chosen. The first is at an intersection of axis \underline{V}_1 with the boundary of the SIR ellipsoid. The second is a point in the intersection of the $\underline{V}_1 - \underline{V}_{M+1}$ plane, the SIR ellipsoid, and the PSD ellipsoid.

restrictive than the PSD constraint along \underline{V}_1 , the major axis. We find

$$\underline{\mathbf{H}}_{(k)} = \begin{cases} \sqrt{w_k(1-\eta_k)(l_1 + \sigma^2)}\underline{V}_1 & \text{CM-DFR} \\ \sqrt{\frac{w_k}{\eta_k}(1-\eta_k)\sigma^2}\underline{V}_1 & \text{Suc. Cancel.} \end{cases} \quad (63)$$

which by Theorem 1 maximizes the largest eigenvalue of $\mathbf{H}_{(k)}$ subject to the SIR constraint.

The second choice is motivated by the fact that a point that lies on the boundary of the PSD constraint will force the $(M+1)$ th-largest eigenvalue of $\mathbf{H}_{(k)}$ to be zero, i.e., the rank of $\mathbf{H}_{(k)}$ will be equal to M which is the rank of $\mathbf{H}_{(k+1)}$. Over all of the possible points lying within the intersection of the two constraints as well as on the boundary of the PSD constraint, we choose one that is nearest to the point chosen in (63). The idea is to minimize the rank of $\mathbf{H}_{(k)}$ while at the same time make its largest eigenvalue as large as possible. Over the set of two-dimensional slices formed by the major axis and one of the other axes, Lemma 4 gives us this point. Using (d'_1, d'_M) from this lemma, our second possible choice if $\underline{\mathbf{H}}_{(k)} = \underline{V}_1 d'_1 + \underline{V}_M d'_M$. The required bandwidth for $\mathbf{H}_{(k)}$ is calculated for both possibilities, and the $\underline{\mathbf{H}}_{(k)}$ that yields the lesser value is chosen.

The method of signal design we have developed avoids exhaustive searches. We do not evaluate and compare the bandwidths associated with a large number of candidate $\underline{\mathbf{H}}_{(k)}$ at each stage in our systematic construction of the correlation matrix. Instead, we carefully consider at most two possible values for $\underline{\mathbf{H}}_{(k)}$ at each stage. Hence, the computational complexity is dominated by the evaluation of at most two spectral decompositions per stage. A quick computation of the signals at the base station is paramount for enabling effective adaptation to changes in the operating conditions as may be caused by users entering and leaving the system, fading, etc.

Before we conclude this section, we address the issue of decoding order. For uncoded systems, users must be detected in the decreasing order of their QoS (i.e., $w_k \eta_k$) to mitigate error propagation effects [13]. For coded systems (and here we limit ourselves to the random coding argument where the order of decoding has, in principle, no effect on error propagation as described earlier), recall that the QoS constraint η_k denotes the

fraction of the k th user's power that is needed for reliable transmission. The smaller the η_k , the greater is user k 's excess power over what is necessary for reliable transmission in the absence of interfering users. Thus we propose the decoding order to be in decreasing order of $(1 - \eta_k)$. This allows users with excess power, who can most afford to combat interfering users, to be decoded earlier. We have found through an extensive set of numerical examples that such an order yields signal sets with consistently lower bandwidths than other orders.

V. NUMERICAL EXAMPLES

In this section, we describe several examples to illustrate the potential for a substantial savings in bandwidth that result from using BEMA. We first obtain a rule-of-thumb for a choice of received power disparities (cf. [16] where the same rule of thumb is used).

If all users transmit with the same power w_t their received powers depend primarily on their distances from the base station. The received power of the k th user can be approximated by the following path-loss formula [17]:

$$w_k = \kappa_0 r_k^{-\nu} w_t \quad (64)$$

where $r_k \in [0, 1]$ is the normalized distance of user k from the base station, ν is an attenuation exponent, and κ_0 is an adjustment factor. The value of ν ranges from $\nu = 2.0$ in free space to $\nu \approx 4.3$ in an open or urban area. If we assume further that the K users are uniformly distributed across a circular cell, then the received power of the k th user is given by

$$w_k = \kappa_0^{-1} \left(\frac{K+1-k}{K+1} \right)^{\nu/2} w_t \quad (65)$$

where the users have been ordered from strongest to weakest. We define the SNR of the system to be that of the weakest user (the user at the cell boundary)

$$\text{SNR} = \kappa_0^{-1} (K+1)^{-\nu/2} \frac{w_t}{N_0}. \quad (66)$$

The SNR of the k th user is thus equal to $\text{SNR} \cdot (K+1-k)^{\nu/2}$, where $\nu/2 \in [1.0, 2.15]$. This means that, on average, the users' received powers exhibit a linear to quadratic power disparity at the receiver.

A. Bandwidth Versus the Number of Users

Figs. 5 and 6 depict the bandwidth needed for BEMA as a function of the number of users for linear and quadratic received power disparities, respectively. In these examples, every user is assigned the same SIR constraint. This symmetric SIR constraint is enforced by requiring $\gamma_k \geq \beta = w_K / \frac{N_0}{2T}$ for all k (i.e., $\eta_k = w_K / w_k$ for all k). For the sake of comparison, we include the OOMA upper bound, the ZF-DFR lower bound (cf. Section II-D-1), and the minimum bandwidth required for TDMA.³ In the case of BEMA, Figs. 5 and 6 depict the bandwidth versus number of users for the CM-DFR, the ZF-DFR,

³The minimum bandwidth for TDMA was obtained in [1] (in this form of TDMA, the signals are constrained to be nonoverlapping in time within the symbol duration but not necessarily of equal duration) and is given by

$$B_{\text{TDMA}} = \frac{1}{2T} \sqrt{\frac{\left(\sum_{k=1}^K w_k^{1/3} \right)^3}{\sum_{k=1}^K w_k}}. \quad (67)$$

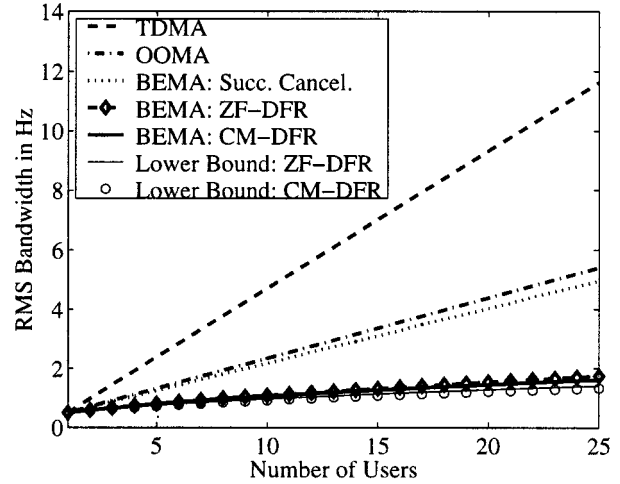


Fig. 5. RMS bandwidth versus the number of users, with $w_k = K - k + 1$, $\text{SNR} = 10 \log_{10}(N_0^{-1}) = 10$ dB, $T = 1.0$, and $\eta_k = w_k^{-1}$.

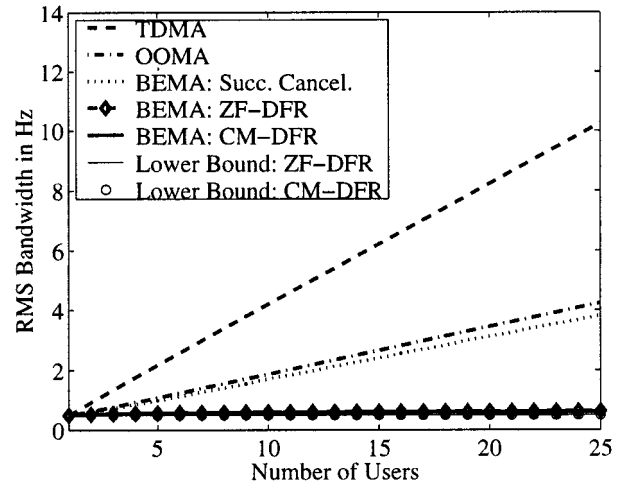


Fig. 6. RMS bandwidth versus the number of users, with $w_k = (K - k + 1)^2$, $\text{SNR} = 10 \log_{10}(N_0^{-1}) = 10$ dB, $T = 1.0$, and $\eta_k = w_k^{-1}$. Note that the ZF-DFR lower bound is only barely distinguishable from BEMA: ZF-DFR and BEMA: CM-DFR.

and the successive-cancellation-based DFR. In Fig. 5, we let $w_k = K - k + 1$ and $T = 1.0$ second so that the SIR constraint becomes $\gamma_k \geq N_0^{-1}$ and (65) and (66) can be combined to yield $\text{SNR} = 10 \log_{10}(N_0^{-1})$ decibels. It is evident that BEMA provides substantial savings in bandwidth over OOMA and TDMA and this savings is most pronounced for the CM-DFR. For example, if $\text{SNR} = 10$ dB, then supporting 20 users with OOMA requires more than three times the bandwidth of BEMA with the CM-DFR (4.39 Hz versus 1.45 Hz). Moreover, note that the bandwidth needed for the ZF-DFR is only slightly more than the unachievable lower bound of Section II-D1, thereby implying that not only can the lower bound be tight, but also that the proposed signal design method can yield signal sets with bandwidth very close to the minimum required bandwidth. For the case of quadratic power disparity in Fig. 6, the gains of BEMA signal design over the OOMA upper bound are even more pronounced.

When power imbalances are high (cf. Fig. 6), our signal design method tends to make the waveforms similar for all users.

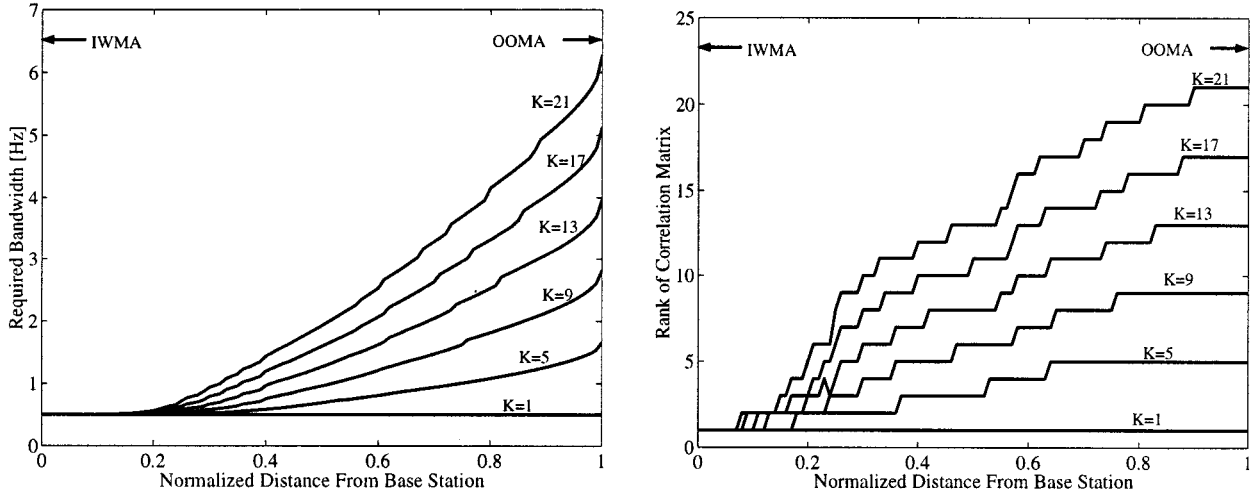


Fig. 7. RMS bandwidth versus normalized distance from base station for equal-power users, $\text{SNR} = 10 \log_{10}(N_0^{-1}) = 6$ dB, $T = 1.0$, and $\eta_k = r^2$.

This follows directly from the observation in Section IV concerning Category 2. That is, the PSD constraint subsumes the SIR constraint when η_k , which is equal to w_K/w_k in this example, is small enough. The result is an $\mathbf{H}_{(k)}$ whose rank is equal to that of $\mathbf{H}_{(k+1)}$. If, on the other hand, $\eta_k = w_K/w_k$ is large enough, then the SIR constraint subsumes the PSD constraint as described in Category 1 in Section IV. Hence, the rank of $\mathbf{H}_{(k)}$ is one greater than the rank of $\mathbf{H}_{(k+1)}$.⁴ If η_k tends to unity for each user, $\mathbf{H}_{(k)}$ for each user gracefully approaches the zero vector. This means that as the power imbalances shrink, BEMA signal design will yield orthogonal signals.

B. Equal Received Powers

In this example, we consider the scenario in which users with equal transmit powers are situated on a ring of normalized radius $r \in [0, 1]$ (if $r = 1$ they would be on the boundary of the cell). A symmetric QoS is imposed where the common SIR constraint is that which results from an isolated user transmitting with the same power from the boundary of the cell ($r = 1.0$) so that $\eta_k = r^\nu$ for all k . Let $\nu = 2$. The closer the users are to the base station, the higher the bandwidth savings for BEMA relative to OOMA. This is because the excess received power of each user relative to the symmetric QoS constraint is higher for smaller r . This is evident in Fig. 7 when the CM-DFR is used for several values of k and an SNR of 6 dB (the plots for other SNRs show similar behavior). Also depicted in Fig. 7 is the rank of the associated correlation matrices. Note that for sufficiently small r , the rank is 1 so that BEMA reduces to IWMA. As r grows sufficiently close to 1, the correlation matrix is full-rank, and when $r = 1$, BEMA reduces to OOMA.

⁴Note, however, that since the bandwidth depends on the actual eigenvalues and not just the rank of the matrix, it is possible for the rank to be increasing while still keeping a rein on the bandwidth. This is illustrated by the similar performances of the ZF-DFR and the CM-DFR in Figs. 5 and 6. The correlation matrix for BEMA with the ZF-DFR is always full-rank, but in these examples its smaller eigenvalues are *significantly* less than the larger eigenvalues.

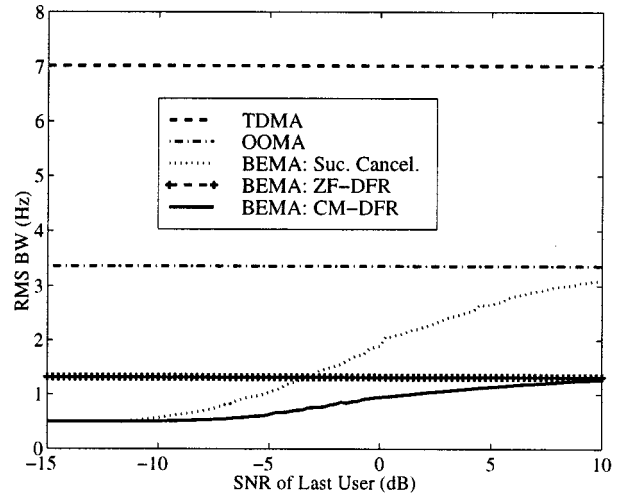


Fig. 8. RMS bandwidth versus $\text{SNR} = 10 \log_{10}(N_0^{-1})$ decibels, with $K = 15$, $w_k = K - k + 1$, $T = 1.0$, and $\eta_k = w_k^{-1}$.

C. The Effect of SNR on Signal Design

We consider again the case of linear disparity in the received powers, and study the effect of varying the noise power. We fix $K = 15$. The symmetric QoS constraint is given as $\gamma_k \geq N_0^{-1}$. Fig. 8 compares the performances of the various receivers as a function of the SNR. Again, BEMA with the CM-DFR requires the least bandwidth over the entire range. Note that our signal design method also consistently maintains the relative performances between the DFR's (for a fixed signal set) even for their respective optimal signal sets.

It is seen in Fig. 8 that the required bandwidths for BEMA with the CM-DFR and the successive-cancellation-based DFR are both very dependent on the SNR since noise power plays a significant role in the signal design for these receivers. At higher values of SNR, the interference is dominated by the interfering users, while at lower values of SNR it is dominated by the noise power. On the other hand, BEMA with the ZF-DFR requires a bandwidth that is independent of SNR. Moreover, since the

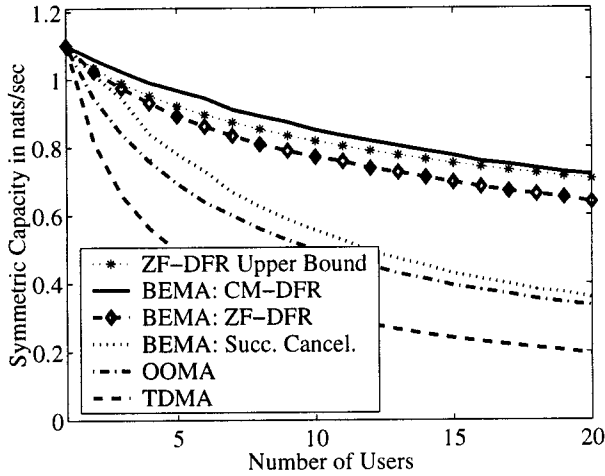


Fig. 9. Symmetric capacity versus the number of users, with rms bandwidth equal to 1 Hz, $w_k = K - k + 1$, $\text{SNR} = 10 \log_{10}(N_0^{-1}) = 3$ dB and $\eta_k = w_k^{-1}$, and $\eta_k = w_k^{-1}$.

ZF-DFR forces the interference to zero, its performance is comparable to that of the CM-DFR for high SNR but distinctly inferior for low SNR. In contrast, successive cancellation ignores the effects of interfering users, so that it compares well with the CM-DFR at low SNR but degrades significantly for high SNR. In any case, BEMA with any one of the three receivers yields substantial savings in bandwidth relative to OOMA and TDMA.

D. User Capacity

In this section, we fix the available bandwidth and depict the number of users that can be supported (user capacity) for a given symmetric (worst user's) capacity constraint.

For a fixed bandwidth, we calculate the symmetric capacity that is achievable with signal design for a given set of users whose relative powers are fixed. In general, as the number of users is increased, the signaling interval must be increased so that the required bandwidth does not grow beyond what is available. This reduces the symmetric capacity since it is strictly decreasing in T . The better the signal design, the less T has to be increased, and hence the less the symmetric capacity is reduced. The ZF-DFR is easiest to work with because its signal design is independent of T . For the CM-DFR and the successive-cancellation-based DFR, we iteratively obtain the signal sets to find the value of T for which the bandwidth is equal to the available bandwidth. For fixed unit bandwidth, the results are shown in Fig. 9, including the upper and lower bounds of Section II-D1 and TDMA. From this figure we see that for a symmetric capacity of 0.8 nats/s, OOMA can support three users whereas BEMA with CM-DFR can support 13 users. Note also that BEMA: ZF-DFR closely tracks its upper bound (deduced from the result in Section II-D1).

Since it may be impossible to dynamically change the signaling interval in practice, the above example should be viewed as a tool for determining a good signaling rate at the system design stage. For example, suppose that the worst case distribution of received powers that can be expected is linear. Then, with the freedom of adjusting the signaling rate, we can find

the maximum number of users that can be supported for a given QoS subject to a bandwidth constraint. The better the design, the greater the number of users that can be supported. Once an operating point is chosen, say a QoS of 0.8 nats/s and a maximum of 13 supportable users, the corresponding signaling interval T can be fixed. If either the disparity of the 13 users increases or if there are less than 13 active users (still with linear disparity), then all users will still be supportable without modifying T .

VI. CONCLUSIONS

The BEMA strategy relies on a QoS-based signal design for nonlinear receivers and was introduced in [1]. As described therein, these signals are to be continually evaluated at a base station so as to adapt to changes in operating conditions such as users entering or leaving the system, changes in power levels due to user mobility, fading, etc. The vector representations of the designed signals are subsequently communicated to the transmitters via a feedback channel. To enable fast adaptation, signal design methods are required to be computationally efficient. The quality-of-service (QoS) based approach is one wherein the reception quality (measured in terms of signal-to-interference ratio (SIR)) is required to be above a certain (possibly distinct) threshold for each user. Under such SIR constraints, the signals are designed to be bandwidth-efficient in that they conserve the bandwidth of the superposition of the users' signals to the extent possible. While [1] obtained bandwidth-efficient signals with respect to the strict bandwidth measure, this paper obtains time-limited signals that are bandwidth-efficient in the rms sense for each one of three high-performance decision-feedback receivers. As in [1], we obtain very substantial savings in bandwidth relative to the more common multiaccess techniques such as TDMA, IWMA, and OOMA. In contrast to the strict bandwidth criterion, however, where the rank of the signal correlation matrix has to be conserved, the rms (or other nonstrict) bandwidth measures require a proper selection of the distribution of the eigenvalues of that matrix. This paper provides several technical results on certain eigenvalue optimization problems in this regard.

APPENDIX

MINIMIZING THE $(M+1)$ th-LARGEST EIGENVALUE

Before proving the result on minimizing the $(M+1)$ th-largest eigenvalue of $\mathbf{H}_{(k)}$ of Theorem 2, we must consider several preliminaries.

Lemma 5: Given the function

$$f(y, \mu) = \begin{cases} w_k y^2 + (1 - y^2)\mu - 2\sqrt{\alpha}y\sqrt{1 - y^2}\sqrt{\mu + \sigma^2} & \text{CM-DFR} \\ w_k y^2 + (1 - y^2)\mu - 2\sqrt{\alpha}y\sqrt{1 - y^2}\sqrt{\mu} & \text{ZF-DFR and PSD constraint} \\ w_k y^2 + (1 - y^2)\mu - 2\sqrt{\alpha}y\sqrt{1 - y^2}\sqrt{\sigma^2} & \text{Suc. Cancel.} \end{cases} \quad (68)$$

where $y \in [0, 1]$, $w_k > 0$

$$\mu \in \begin{cases} [-\sigma^2, \infty) & \text{CM-DFR} \\ [0, \infty) & \text{ZF-DFR and PSD constraint} \\ (-\infty, \infty) & \text{Suc. Cancel.} \end{cases} \quad (69)$$

and, as per the discussion in Section II-D

$$\alpha \in \begin{cases} (0, w_k) & \text{CM-DFR or ZF-DFR} \\ [w_k, w_k] & \text{PSD constraint} \\ (0, \infty) & \text{Suc. Cancel.} \end{cases} \quad (70)$$

so that $\alpha > 0$. Then

1) For all but the successive-cancellation case, $\partial f/\partial \mu$ has only one stationary point. It corresponds to a minimum and is given by the function

$$\mu_o(y) = \begin{cases} ((\alpha + \sigma^2)y^2 - \sigma^2)(1 - y^2)^{-1} & \text{CM-DFR} \\ \alpha y^2(1 - y^2)^{-1} & \text{ZF-DFR and PSD constraint.} \end{cases} \quad (71)$$

This function is strictly increasing in y with $\mu_o(0) = -\sigma^2$ and $\lim_{y \rightarrow 1} \mu_o(y) = \infty$ for the CM-DFR, while $\mu_o(0) = 0$ and $\lim_{y \rightarrow 1} \mu_o(y) = \infty$ for the ZF-DFR and the PSD constraint. For successive cancellation, $\partial f/\partial \mu$ is strictly positive except at $y = 1$ where it is zero.

2) $\partial f/\partial y$ has only one stationary point and it corresponds to a minimum. It is given by the function

$$y_o(\mu) = \sqrt{2} \left(4 + X^2 + X \sqrt{4 + X^2} \right)^{-1/2} \quad (72)$$

where

$$X = \begin{cases} (w_k - \mu)/\sqrt{\alpha(\sigma^2 + \mu)} & \text{CM-DFR} \\ (w_k - \mu)/\sqrt{\alpha\mu} & \text{ZF-DFR and PSD constraint} \\ (w_k - \mu)/\sqrt{\alpha\sigma^2} & \text{Suc. Cancel.} \end{cases} \quad (73)$$

This function is strictly increasing in μ and satisfies $y_o(-\sigma^2) = 0$ and $\lim_{\mu \rightarrow \infty} y_o(\mu) = 1$ for the CM-DFR, $y_o(0) = 0$ and $\lim_{\mu \rightarrow \infty} y_o(\mu) = 1$ for the ZF-DFR or the PSD constraint, and $\lim_{\mu \rightarrow -\infty} y_o(\mu) = 0$ and $\lim_{\mu \rightarrow \infty} y_o(\mu) = 1$ for successive cancellation.

3) For the CM-DFR and the ZF-DFR we have that $\mu \geq \mu_o(y_o(\mu))$ with strict inequality except when $\mu = -\sigma^2$ for the CM-DFR and $\mu = 0$ for the ZF-DFR. For the PSD constraint it is always true that $\mu = \mu_o(y_o(\mu))$.

Proof: We will consider only the CM-DFR. Part 1) is straightforward to show, and Part 2) is shown in essentially the same way that (44) was derived. Thus we concentrate on the most interesting case, Part 3). Using (71), Part 3) can be equivalently stated as

$$y_o^2(\mu) \leq (\mu + \sigma^2)/(\mu + \alpha + \sigma^2). \quad (74)$$

Hence, we see that when $\mu = -\sigma^2$, equality holds. (Note also that $y_o(\mu)$ is zero only when $X = \infty$, and this is possible only for $\mu = -\sigma^2$.) Recall from (70) that for the CM-DFR $\alpha = w_k(1 - \eta_k) > 0$, and define $Y = \mu + \sigma^2 \geq 0$ and $Z = \eta_k w_k - \mu$. Using these definitions and the expression for $y_o(\mu)$ in Part 2), (74) can be restated as

$$\frac{1}{2\alpha} Y \left(2 + X^2 + X \sqrt{4 + X^2} \right) \geq 1. \quad (75)$$

Now, since $X = (\alpha + Z)/\sqrt{\alpha Y}$, it is possible after some algebraic manipulation to show that this becomes

$$g \triangleq \frac{1}{2\alpha^2} \left(2Y\alpha + (\alpha + Z)^2 + (\alpha + Z) \cdot \sqrt{4Y\alpha + (\alpha + Z)^2} \right) \geq 1. \quad (76)$$

To show that this is always true, we must consider four possible cases.

For the first case, suppose that $Z \geq 0$. This implies that $\alpha + Z \geq \alpha > 0$ so that $(\alpha + Z)^2 \geq \alpha^2$. Moreover, since $Y > 0$ (the case $Y = 0$, i.e., $\mu = -\sigma^2$, was already discussed), we find that

$$g > (2\alpha^2)^{-1}(0 + \alpha^2 + \alpha\sqrt{0 + \alpha^2}) = 1.$$

In the second case we have that $Z < 0$ and $\alpha = -Z$. Then $\alpha + Z = 0$ and $g = Y/\alpha = Y/(-Z)$. But the latter equals $\mu/(\mu - \eta_k w_k) + \sigma^2/(\mu - \eta_k w_k)$, where, since $-Z > 0$, the first term is greater than unity and the second term is positive. Thus we find that for the second case $g > 1$ is also true. Note also that the last step indicates that $Z < 0$ implies that $Y > -Z$; this fact will be used in proving the next two cases.

For the third case, we consider $Z < 0$ and $\alpha > -Z$ so that $\alpha + Z > 0$. Since it is also true that $Y > -Z > 0$, we find that

$$g > \frac{1}{2\alpha^2} \left(2(-Z)\alpha + (\alpha + Z)^2 + (\alpha + Z) \cdot \sqrt{4(-Z)\alpha + (\alpha + Z)^2} \right) = 1. \quad (77)$$

The fourth and final case is when $Z < 0$ and $\alpha < -Z$, so that $\alpha + Z < 0$ and $Y > -Z > \alpha > 0$. We can then rewrite g as

$$g = \frac{1}{2\alpha^2} \left(2Y\alpha - (\alpha + Z)^2 \left(-1 + \left(1 + \frac{4Y\alpha}{(\alpha + Z)^2} \right)^{1/2} \right) \right) \quad (78)$$

since here $\sqrt{(\alpha + Z)^2} = -(\alpha + Z)$. Now, to arrive at a contradiction, suppose that $g < 1$. Since $(\alpha + Z)^2 > 0$ we find this to be equivalent to $\Psi(1 - \alpha/Y) + 1 < \sqrt{1 + 2\Psi}$ where $\Psi \triangleq 2Y\alpha/(\alpha + Z)^2$, a positive number. Since $Y > \alpha > 0$, we can square both sides without changing the direction of the inequality. After some algebra we arrive at $\Psi(\frac{Y-\alpha}{Y})^2 < 2\alpha/Y$. We can replace Ψ with its definition to eventually yield the equivalent statement $|Y - \alpha| < |\alpha + Z|$. But this is a contradiction since

$$|Y - \alpha| = |Y - (-Z) + (-Z - \alpha)| \quad (79)$$

$$= |Y + Z| + |\alpha + Z| > |\alpha + Z| \quad (80)$$

where the second line is a result of $Y > -Z$ and $\alpha + Z < 0$. Thus our assumption for this final case that $g < 1$ was false, and so $g \geq 1$ as desired. \square

Corollary 1: The minimum of f on the set of (y, μ) such that $y \in [0, 1]$ and $\mu \in [l_M, l_1]$, where $l_M \geq 0$, occurs at the point $(y_o(l_M), l_M)$.

Proof: Fig. 10 may help the reader follow this proof. Choose any (y, μ) in the appropriate set and suppose that it yields the minimum of f . But $f(y, \mu) > f(y_o(\mu), \mu)$ unless $y = y_o(\mu)$ by the second result of Lemma 5. The first and third results of the same lemma tell us that

$$f(y_o(\mu), \mu) > f(y_o(\mu), \max\{l_M, \mu_o(y_o(\mu))\})$$

unless $\mu = \max\{l_M, \mu_o(y_o(\mu))\}$. But over the region of interest, this occurs only when $\mu = l_M$ as indicated by the third part of Lemma 5. Thus only the point $(y_o(l_M), l_M)$ yields the minimum of f . \square

We can finally prove Theorem 2.

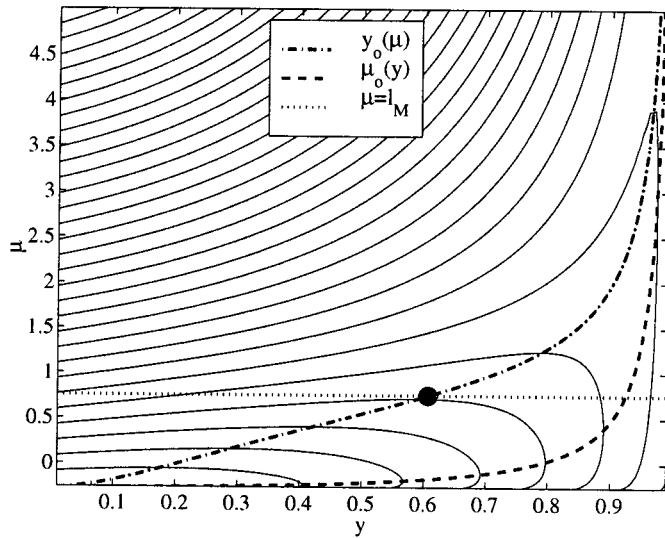


Fig. 10. A contour plot of the “valley” formed by $f(y, \mu)$ when $w_k = 0.9797$, $\sigma^2 = 0.2714$, $l_M = 0.75$, and $\alpha = 0.1730$. The indicated point, $(y_0(l_M), l_M)$, is the argument that minimizes $f(y, \mu)$ over the constraint region.

Proof: We will specifically consider the CM-DFR, the other constraints being treated in a similar fashion. Choosing \underline{D} as in (23) of Lemma 2 we now seek to minimize the function $f(y, \underline{Z}) = w_k y^2 + \underline{Z}^T \mathbf{H}_{(k+1)} \underline{Z} - 2|y| \sqrt{\alpha} \cdot \sqrt{\underline{Z}^T \mathbf{H}_{(k+1)} \underline{Z} + \sigma^2 \underline{Z}^T \mathbf{V} \mathbf{V}^T \underline{Z}}$ (81) over the set of y, \underline{Z} such that $y^2 + \underline{Z}^T \underline{Z} = 1$, for this yields the smallest eigenvalue of $\mathbf{H}_{(k)}$. This is symmetric in y , so we assume without loss of essential generality that $y \in [0, 1]$. Let $\bar{\mathbf{V}}$ denote the matrix containing a set of column vectors so that $[\mathbf{V} \bar{\mathbf{V}}]$ is an $K - k \times K - k$ orthogonal matrix; this is always possible since the columns of \mathbf{V} are orthonormal. Note that if we choose \underline{Z} to be any one of the columns of $\bar{\mathbf{V}}$, say \underline{U}_1 , then $f(y, \underline{U}_1) = w_k y^2$ results since $\mathbf{V}^T \underline{U}_1 = 0$. Setting $y = 0$ then yields $f(0, \underline{U}_1) = 0$. Since $\mathbf{H}_{(k)}$ is of a form that forces it to be positive-semidefinite, we know that this has yielded the smallest eigenvalue of $\mathbf{H}_{(k)}$. Now, again by the Rayleigh–Ritz theorem, we know that the second smallest eigenvalue of $\mathbf{H}_{(k)}$ is given the minimization of $f(y, \underline{Z})$, subject to $y^2 + \underline{Z}^T \underline{Z} = 1$ and $[y \ \underline{Z}^T]$ being orthogonal to $[0 \ \underline{U}_1^T]$. But choosing \underline{Z} to be some column of $\bar{\mathbf{V}}$ other than \underline{U}_1 , this time say \underline{U}_2 , then $f(0, \underline{U}_2)$ is also zero. Proceeding similarly, we find that the $K - k - M$ smallest eigenvalues of $\mathbf{H}_{(k)}$, each of which is guaranteed to be zero, are yielded by choosing \underline{Z} to be the $K - k - M$ columns of $\bar{\mathbf{V}}$.

To find the next smallest eigenvalue, which is also the $(M + 1)$ th-largest eigenvalue, we minimize $f(y, \underline{Z})$ subject to $y^2 + \underline{Z}^T \underline{Z} = 1$ and $[y \ \underline{Z}^T][0 \ \bar{\mathbf{V}}^T]^T = \mathbf{0}^T$. The latter constraint is equivalent to saying that \underline{Z} must be a linear combination of the rows of $\bar{\mathbf{V}}$. This, along with the fact that $\underline{Z}^T \underline{Z} = 1 - y^2$, tells us that $\underline{Z}^T \mathbf{V} \mathbf{V}^T \underline{Z} = 1 - y^2$ and $\underline{Z}^T \mathbf{H}_{(k+1)} \underline{Z} \in [(1 - y^2)l_M, (1 - y^2)l_1]$. Denoting the latter term by the term $(1 - y^2)\mu$ where $\mu \in [l_M, l_1]$, we seek to minimize

$$f(y, \mu) = w_k y^2 + (1 - y^2)\mu - 2\sqrt{\alpha} y \sqrt{1 - y^2} \sqrt{\mu + \sigma^2} \quad (82)$$

over $y \in [0, 1]$ and $\mu \in [l_M, l_1]$. But by Lemma 5 and Corollary 1 we know that $\mu = l_M$ and $y = y_0(l_M)$ yields the minimum. Thus $\underline{Z} = \sqrt{1 - y_0(l_M)} \underline{V}_M$. Following a line of reasoning similar to the last paragraph of the proof of Theorem 1, this becomes $\underline{Z} = \sqrt{\alpha(l_M + \sigma^2)} \underline{V}_M$. \square

ACKNOWLEDGMENT

The authors wish to thank the anonymous reviewers for their helpful comments, particularly one reviewer’s suggestion that perhaps the arithmetic-geometric inequality could be used to derive a lower bound.

REFERENCES

- [1] M. K. Varanasi and T. Guess, “Bandwidth-Efficient Multiple Access (BEMA): A new strategy based on signal design for multiuser receivers under Quality-of-Service constraints,” *IEEE Trans. Commun.*, May 1998, submitted for publication.
- [2] R. S. Cheng and S. Verdú, “Capacity of root-mean-square bandlimited Gaussian multiuser channels,” *IEEE Trans. Inform. Theory*, vol. 37, pp. 453–465, May 1991.
- [3] D. Parsavand and M. K. Varanasi, “RMS bandwidth constrained signature waveforms that maximize the total capacity of PAM-synchronous CDMA channels,” *IEEE Trans. Commun.*, vol. 44, pp. 65–75, Jan. 1996.
- [4] M. Rupf and J. L. Massey, “Optimum sequence multisets for synchronous code-division multiple-access channels,” *IEEE Trans. Inform. Theory*, vol. 40, pp. 1261–1266, July 1994.
- [5] P. Viswanath and V. Anantharam, “Optimal sequences and sum capacity of synchronous CDMA systems,” *IEEE Trans. Inform. Theory*, vol. 45, pp. 1984–1991, Sept. 1999.
- [6] M. K. Varanasi and E. A. Fain, “Optimum signal design and power control for multiuser wireless communications under location-invariant bandwidth constraints,” in *Proc. 36th Allerton Conf. Communication, Control, and Computing*, Sept. 1998, pp. 556–565.
- [7] M. K. Varanasi and T. Guess, “Bandwidth-efficient multiple-access via signal design for decision-feedback receivers: Towards an optimal spreading-coding trade-off,” in *Proc. IEEE Global Telecommunications Conf.: Communication Theory Mini-Conf.*, Phoenix, AZ, Nov. 3–8, 1997, pp. 159–165.
- [8] —, “Optimum decision feedback multiuser equalization with successive decoding achieves the total capacity of the Gaussian multiple-access channel,” in *Proc. 31st Asilomar Conf. Signals, Systems, and Computers*, Nov. 1997, pp. 1405–1409.
- [9] P. Viswanath, V. Anantharam, and D. Tse, “Optimal sequences, power control and user capacity of synchronous CDMA systems with linear MMSE multiuser receivers,” *IEEE Trans. Inform. Theory*, vol. 45, pp. 1968–1983, Sept. 1999.
- [10] S. Ulukus and R. D. Yates, “Iterative signature adaptation for capacity maximization of CDMA systems,” in *Proc. 36th Allerton Conf. Communication, Control and Computing*, Allerton, IL, Sept. 1998, pp. 506–515.
- [11] M. K. Varanasi and T. Guess, “Bandwidth-Efficient Multiple-Access (BEMA): Signal design with a strict bandwidth criterion under Quality-of-Service constraints,” in *Proc. Int. Symp. Signals, Systems, and Electronics (ISSSE’98)*, Pisa, Italy, Sept. 29–Oct. 2, 1998, pp. 146–151.
- [12] E. A. Fain, “Minimum bandwidth basis functions for the fourth-moment bandwidth measure,” in *IEEE Int. Symp. Information Theory (ISIT’2000)*, Sorrento, Italy, June 2000.
- [13] M. K. Varanasi, “Decision feedback multiuser detection: A systematic approach,” *IEEE Trans. Inform. Theory*, vol. 45, pp. 219–240, Jan. 1999.
- [14] T. Guess and M. K. Varanasi, “Error exponents for maximum-likelihood and successive decoders for the Gaussian CDMA channel,” *IEEE Trans. Inform. Theory*, vol. 46, pp. 1683–1691, July 2000.
- [15] R. A. Horn and C. R. Johnson, *Matrix Analysis*. Melbourne, Australia: Cambridge Univ. Press, 1993.
- [16] R. R. Muller and J. B. Huber, “Capacity of cellular CDMA systems applying interference cancellation and channel coding,” in *Proc. IEEE Global Telecommunications Conf.: Communications Theory Mini-Conf.*, Phoenix, AZ, Nov. 3–8, 1997, pp. 179–184.
- [17] W. C. Y. Lee, *Mobile Communications Design Fundamentals*. New York: Wiley, 1993.